Effect of detector nonlinearity and image persistence on CARS derived temperatures

Snelling, D. R.; Smallwood, G. J.; Parameswaran, T.

Publisher's version / Version de l'éditeur:

Applied Optics, 28, 15, pp. 3233-3241, 1989

Effect of detector nonlinearity and image persistence on CARS derived temperatures

D. R. Snelling, G. J. Smallwood, and T. Parameswaran

The image persistence of self-scanning photodiode arrays (IPDA) incorporating P-20 phosphor-based intensifiers is shown to make them unsuitable for single-pulse CARS temperature measurements in turbulent combustion. Correcting CARS flame spectra for the nonlinear response of the IPDA detectors increases CARS derived temperatures ≈3–6%. This error is partially offset by correcting for the perturbations in the N_2 vibrational population resulting from stimulated Raman pumping. The effect of these population perturbations on CARS-derived temperatures is determined. CARS flame spectra obtained with uncorrelated pump beams that are corrected for IPDA nonlinearity and stimulated Raman pumping are shown to give temperatures in good agreement with combined thermocouple/sodium line-reversal measurements.

I. Introduction

Single-pulse, broadband CARS (coherent anti-Stokes Raman spectroscopy) is an important diagnostic technique for combustion measurements of temperature and species concentration. The single-pulse capability requires the use of optical multichannel detectors (OMD) such as the intensified silicon intensified target (ISIT) vidicon or, more commonly, the intensified self-scanning photodiode array (IPDA).

Several IPDA detectors incorporating a P-20 phosphor in the image intensifier have been shown to have a nonlinear response and to exhibit an image persistance (lag) that is more pronounced than was commonly realised.[1] This problem appears to be generic to the P-20-based IPDA detectors.[1,2] Although the nonlinearity of the ISIT vidicons was not examined they are likely to behave in a similar way to the IPDA detectors since both incorporate P-20-based image intensifiers that were implicated[1] in the nonlinearity of the IPDA detectors.

Detector image persistence presents a particular problem for single-pulse CARS measurements in turbulent combustion environments. The CARS signal increases markedly with decreasing temperature and this has necessitated the use of multiple-beam techniques[3,4] to extend the dynamic range of the OMDs. With a large dynamic range even weak image persistence can lead to CARS spectral distortion.

For a 10-Hz CARS system the typical image persistence for a P-20-based IPDA is[1] ~0.5–2.0% with the majority of the persistence resulting from CARS exposures prior to the preceding one. Because of the dependence of CARS signal on temperature, the image persistence will result in a residual image that is biased to lower temperatures. In this report we attempt to evaluate the effect of image persistence on CARS-derived temperatures by synthesising purely theoretical spectra that are mixtures of two temperatures. These synthetic spectra are then analyzed to obtain best-fit temperatures to assess the resulting error.

The IPDA nonlinearity that involves a logarithmic fall-off in relative sensitivity with output signal[1,2] appears not to have been considered previously in CARS spectroscopy. Correcting the data for this effect increases the best-fit temperatures by 45–100 K at 1600 K (3–6%).

There have been many comparisons of CARS-derived temperatures with those obtained by other techniques such as thermocouple and sodium line-reversal (see, for example, Ref. 5 and 6 which summarize the earlier work). Some recent comparisons,[7–9] including our own,[10] have claimed 1.0–1.5% accuracy. Thus we were disconcerted to find a nonlinearity whose inclusion resulted in a substantial increase in best-fit temperatures.

In this paper we assess the effect of this IPDA nonlinearity on best-fit CARS temperatures. We also examine the effect of various assumptions in the CARS theory and the fitting procedures on the best-fit temperatures. In particular it appears that stimulated Raman-induced changes in the vibrational state populations are perturbing the CARS spectra which then appear anomalously hot.

There have been relatively few studies of population perturbations in broadband CARS as compared to scanning CARS in which two narrowband lasers are used. Regnier *et al.*,[11] presented a formula for population transfer times for monochromatic lasers and Gierulski *et al.*,[12] have reported measurements of pump-induced population changes in room temperature N_2 using a broadband CARS system. This latter study employed a short focal length focusing lens and the

The authors are with National Research Council of Canada, Division of Mechanical Engineering, Ottawa, Ontario K1A OR6, Canada.

Received 1 March 1989.
0003-6935/89/153233-09$02.00/0.

resultant high peak laser intensities resulted in an apparent vibrational temperature of 2550 K in room temperature N_2.

Detector nonlinearity and stimulated Raman pumping have offsetting effects on CARS-derived temperatures so that neglecting both may produce results that appear reasonable. In this paper we assess the effect of stimulated Raman pumping on CARS-derived temperatures.

II. Experimental Apparatus and Data Reduction

A. CARS Spectrometer

Most of the data presented in this report was collected with the CARS instrument described previously.[10–14] We have recently replaced the USED CARS phase-matching technique employed previously[10–14] with folded BOXCARS[15] phase matching. The CARS spectra were recorded in a premixed flat-flame burner[10] operating on hydrogen/air at an equivalence ratio of 0.574. The measured sodium line-reversal temperature 10 mm above the burner center line was[10] 1593 ± 18 K. We have subsequently verified this measurement by using three different-sized thermocouples to measure the flame temperature.[16] The thermocoupled readings were corrected for radiation and conduction losses although the extrapolation of the data to zero thermocouple diameter greatly reduced the need to know the correction accurately. The final temperature obtained from the thermocouple measurements was 1560 ± 22 K which is in satisfactory agreement with the Na line-reversal measurements. We adopted an average value of 1577 ± 20 K as our best estimate of the temperature 10 mm above the burner centerline.

The data in Refs. 10–14 and the data reported here employing USED CARS phase matching were generated using a Spectra Physics DCR 1A Nd:YAG laser that had a spectra bandwidth of 0.10 ± 0.03 cm^{-1} with the intracavity etalon and 0.69 ± 0.05 cm^{-1} with the etalon removed. The laser was subsequently rebuilt (the remeasured bandwidths are 0.22 ± 0.04 cm^{-1} (etalon in) and 0.67 ± 0.10 cm (no etalon)) and used for the folded BOXCARS phase-matching experiments.

For the USED CARS experiments in Ref. 10, a 200-mm focal length CARS focusing lens was used and the laser energies were 30 mJ (pump) and 5 mJ (Stokes). The laser focal spot sizes (aperture diam. to pass 50% of the beam) were 45 μm (pump) and 75 μm (Stokes).

For the USED CARS experiments discussed in Sec. IIIC and shown in Fig. 5 the lens focal length was 300 mm, the pump laser energy 70 mJ, the Stokes laser energy 13–22 mJ, and the laser focal spot sizes 75 μm (pump) and 70 μm (Stokes).

For the folded BOXCARS experiments the lens focal length was 300 mm, the total pump laser energy 50 mJ, the Stokes laser energy 10 mJ, and the laser focal spot sizes 75 μ (pump) and 60 μm (Stokes).

B. CARS Theory and Data Reduction

The accuracy of CARS-derived temperatures is largely determined by the synthetic theoretical spectra generated for analysis of the data. The theoretical models and the computer program used to calculate the synthetic CARS spectra have been described in some detail[10,17] and they will only be summarized here.

The effect of collisional narrowing of Raman lines[18] and cross-coherence terms that arise[19,20] in the laser convolution of CARS intensity are included as options in the calculation of CARS spectra. The theoretical model used previously[10] has been modified to include the O and S branches of N_2. The effect of these and other small changes[17] to the computer model was evaluated by fitting a theoretical 1550-K spectrum generated by the earlier program[10] with a library calculated with the modified program. The best-fit temperature obtained was 1558.8 K showing that the refinements to the program had resulted in a change of 8.8 K.

In conventional flame CARS spectroscopy Doppler broadening is neglected and the Raman lines are assumed to have Lorentzian shapes. When Doppler broadening is significant a Voigt profile describes the line shape more accurately. Henesian and Byer[21] have provided a generalized expression for the CARS susceptibility using Voigt profiles expressed in terms of complex probability functions. In the updated version[17] of our CARS theoretical spectrum generating program, an option has been provided to use a Voigt line shape function. At atmospheric pressure and flame temperatures around 1500 K it is often not clear whether collisional narrowing due to overlap of pressure broadened lines or Doppler broadening plays a more important role. As a test we have fitted 1550-K spectrum of N_2 obtained with the isolated line model with cross-coherence (IT) against libraries with (i) collision narrowing and cross-coherence (GT) and (ii) with isolated line and Voigt profile (ITV). The GT model gave a best-fit temperature of 1554 K and the ITV model gave 1558 K.

This test suggests that, while both the above improvements produce only modest changes in the temperature, the CARS spectrum is perhaps more sensitive to the use of Voigt profile than the inclusion of collisional narrowing for T = 1550 K.

A set of programs for fitting experimental CARS spectra to calculated spectra, including a nonlinear least mean squares fitting scheme, was developed.[17] The calculation of a typical theoretical CARS flame spectrum can take a few hours with a DEC VAX-11/730 computer. Therefore, a method of estimating temperatures by fitting experimental CARS spectra to a precalculated library of theoretical CARS spectra at various temperatures was implemented. The instrument function required to create this library is obtained by fitting room-temperature nitrogen CARS spectra. With this approach less than two seconds of DEC VAX-11/730 CPU time was required to fit a single experimental spectrum. The original[10] four-parameter, asymmetric, Voigt instrument function was expanded[17] optionally to include two terms that

decayed as the reciprocal of the frequency displacement, creating a six-parameter modified Voigt instrument function. The fitting programs were also modified to allow the CARS intensities to be corrected for detector nonlinearity.

III. Results and Discussion

A. Effect of Image Persistence on CARS Temperatures

Image persistence in P-20-based IPDA detectors was shown[1] to contribute about 0.5–2.0% of the signal in a typical CARS system. Most of this image persistence comes from pulses prior to the preceding one and is caused by the slowly decaying components of many earlier CARS signals.

We have modeled the effect of this image persistence on CARS-derived temperatures by synthesizing theoretical spectra that are mixtures of two temperatures. Six synthetic spectral libraries were created by adding 0.5 or 2.0% of 500 K, 700 K, or 1000 K theoretical CARS spectra to a standard library of spectra calculated (for a constant pressure of one atmosphere) at every 100 K, from 300–2100 K. The synthetic spectra were then treated as experimental spectra and fitted to the original library to obtain the best-fit temperatures.

The error in best-fit temperatures that results from adding the image persistence of a cooler spectrum to a hot spectrum increases markedly with temperature as shown in Fig. 1. This occurs because the CARS intensity decreases with increasing temperature, with the peak intensity of a 2100-K spectrum being ~1/1000 that of a 300-K spectrum (assuming constant pressure).

For the same reason the increase in best-fit temperatures that results from adding the image persistence of a hot spectrum to a colder spectrum is negligible. The maximum increase in best-fit temperature observed was 3.3 K and for this reason these data are not presented in Fig. 1.

The image persistence results in time averaging of CARS spectra and the effect on CARS-derived temperatures is similar to that of spatial averaging within the probe volume that has been discussed recently.[22]

The temperature errors (Fig. 1) that result from the admixture of cold spectra are unacceptably large. In a turbulent flame with pockets of cool and hot gases this would result in temperature histograms biased to lower temperatures where the biasing would depend on the particular time history as well as the temperature distribution. In practice it will be difficult to assess quantitatively the effect on CARS-derived temperatures of image persistence since it is long lived (up to several seconds) and many previous CARS signals will contribute. A prototype detector with a faster rare-earth phosphor[1] more suited to CARS temperature measurements in a turbulent environment will greatly reduce these problems.

B. Detector nonlinearity

The effect of correcting a CARS spectral signature for detector nonlinearity is shown in Fig. 2 for a spectrum recorded in the flat-flame burner using the Tracor Northern TN-6132 detector. The correction applied is essentially that shown in Fig. 1 of Ref. 1.

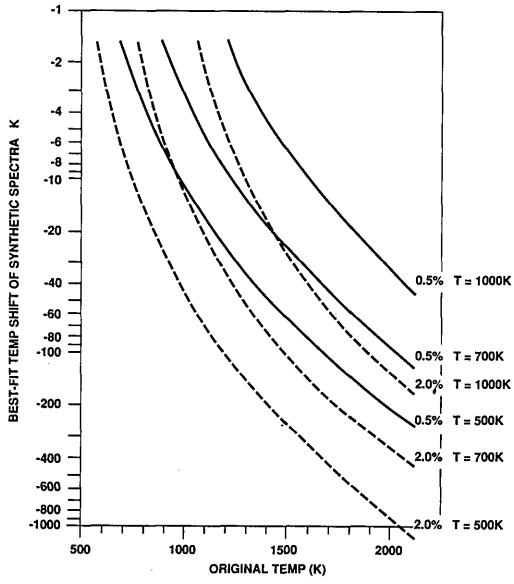

Fig. 1. Image persistence for a Princeton Instruments model IRY-1024 IPDA following an interrupted 10-Hz laser exposure.

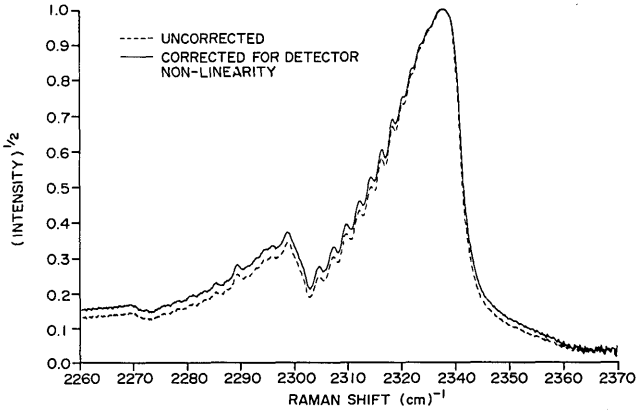

Fig. 2. Effect of correcting for detector nonlinearity on an experimental CARS flame spectrum.

Applying this correction results in best-fit CARS temperatures (see Table I) that are ≈50–100 K hotter at 1600 K. Applying the nonlinear correction destroys the agreement we had previously reported[10] between CARS temperatures and Na line-reversal temperatures.

In an attempt to discover the cause of this discrepancy we investigated the effect of various fitting options and CARS input data on CARS derived temperatures. The data consisted of three experiments, comprising 30 files, each containing 100 single-pulse CARS spectra (0.69 cm^{-1} pump laser bandwidth) recorded in the hydrogen/air flat-flame burner and employing USED CARS phase matching.

The result of this investigation is shown in Table I. For the weighted least mean squares (LMS) fits, the weights assigned to each diode signal were obtained

from the measured detector noise characteristics with an added component for the shot-to-shot variation in the Stokes laser spectral profile[10] (assumed to be 4% in Table I). The Raman linewidth and relaxation rate data used in calculating the theoretical CARS spectra are referenced in Table I.

For entries A–E the four-parameter instrument function was obtained by unweighted fitting of experimental room temperature N_2 spectra to theoretical spectra that were convolved to ±10 Voigt widths (typically ±15 cm^{-1}).

For entry F the fitting program used to obtain the instrument function from the room-temperature nitrogen spectra[17] was modified. Spectral shift was added as a fitting parameter[17] to replace the original strategy of aligning the maximum intensity points in the experimental and synthetic room-temperature N_2 CARS spectra and weighting was used where appropriate.

For entries G and H, the convolution of the theoretical CARS spectra was with the six-parameter modified Voigt instrument function, and the convolution range was extended from ±10 Voigt widths[10] to ±50 cm^{-1} independent of the Voigt parameter. A more accurate nonlinear correction of the IPDA response was employed that resulted in corrections that were ~15% less than for the nonlinear correction employed in entries A–F.

Table I. Effect of CARS theoretical model assumption on best-fit single-pulse CARS temperatures[a]

Code for CARS model used	Average best-fit cars temperature			
	Uncorrected for detector nonlinearity		With nonlinear detector correction	
	Unweighted LMS fit	Weighted LMS fit	Unweighted LMS fit	Weighted LMS fit
A	1541	1509	1639	1632
B	1579	1573	1691	1700
C	1565	1550	1675	1683
D	—	—	1599	1561
E	1570	1550	1679	1675
F	1569	1549	1668	1668
G	1574	1582	1622	1643
H	1570	1574	1618	1633

[a] Except as noted, the synthetic spectra were calculated with collisional narrowing and cross-coherence effects included. The changes in the model and the input parameters are listed below.

A Raman linewidths and exponential gap model for relaxation rate data taken from Ref. 23.

B Raman linewidths and exponential gap model relaxation rate data taken from Ref. 24.

C Raman linewidths augmented by 9% to account for the additional broadening effect of water vapor.[25]

D Nonresonant susceptibility increased by 50%.

E More accurate version[26] of exponential gap model for relaxation rate data implemented with 9% augmentation for water vapor.

F Fitting programs modified to include more accurate fit to room-temperature N_2 spectra (see text). The Raman linewidths were those of entry E.

G The theoretical spectra were convolved with a six-parameter instrument function convolved to ±50 cm^{-1} and a more accurate nonlinear correction of the IPDA response was employed (see text). The Raman linewidths were those of entry E.

H Same as G except the synthetic flame spectra were calculated with the effects of cross-coherence and Doppler broadening (Voigt profile) included.

The theoretical spectral libraries used to generate the best-fit temperatures for entries A–G in Table I were calculated with the effects of collisional narrowing and cross-coherence included. The pump laser bandwidth was 0.69 cm^{-1}. Entry H was generated with the effects of cross-coherence and Doppler broadening included.

The best-fit unweighted CARS temperatures in Table I are ~50–100 K hotter when the nonlinear correction is applied. The temperature shifts noted previously,[10] when weighted as compared to unweighted LMS fitting was applied, are frequently observed for the uncorrected fits in Table I but are largely absent when the nonlinear correction is applied. Since, with weighting, the lower CARS signals are accorded relatively greater importance in the LMS fitting procedure, this suggests that applying the nonlinear correction results in a CARS spectrum where the high and low signal features are consistent with a single temperature.

We have routinely adopted weighted least mean squares (WLMS) fitting of CARS spectra, first, because, the WLMS fit markedly increases the precision of single-pulse CARS temperature measurements.[10] And, second, because an unweighted LMS fit implicitly assumes that the error (variance) associated with an individual diode reading is constant independent of signal level and this clearly is not correct.[5,10,13]

Model A in Table I corresponds to the CARS synthetic spectra used in our earlier study[10] where the N_2 Raman linewidths[23] were taken to be independent of combustion species (i.e., CO_2/N_2 and H_2O/N_2 collisions were assumed to have an effect identical to N_2/N_2 collisions) and the relaxation rate data were obtained from an exponential gap model.[23]

The use of Raman linewidths and state relaxation rates based on more extensive high temperature and pressure N_2 Raman linewidth data[24] increased best-fit temperatures (model B, Table I) by 40–70 K. This increase partly disappeared as, first, the effect of H_2O broadening on N_2 Raman linewidths[25] was included (model C, Table I) and, second, a more accurate empirical expression for the exponential gap relaxation rate model[26] (model E, Table I) was implemented.

During the analysis it became clear that, particularly for the weighted and corrected fits, it was important to fit the low-intensity wings of the instrument function. To accomplish this the six-parameter modified Voigt instrument function was implemented and the convolution range extended. As expected this had a greater effect on the weighted fits as can be seen by comparing the uncorrected best-fit temperatures for F and G in Table I. The reduction in the corrected best-fit temperatures for G as compared to F is in part due to the modified nonlinear correction employed for G. The modified nonlinear correction (G and H) results in smaller increase in best-fit temperatures than the previous correction (A–F). If the experimental flame data are analyzed with the same theoretical slit convolved library both with and without the correction applied, the change in best-fit temperatures is typical-

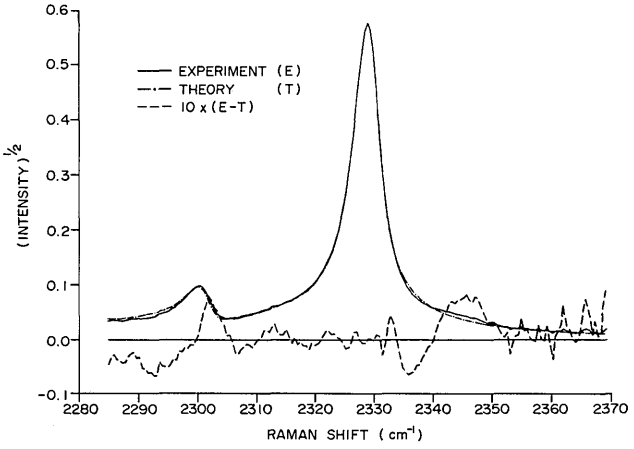

Fig. 3. Comparison of an experimental room-temperature CARS spectrum to a theoretical N_2 CARS spectrum calculated for T_V = 1325 K and T_R = 294 K and convolved with a best-fit six parameter instrument function.

ly 90 K. The smaller temperature increment observed for G and H in Table I when the correction for detector nonlinearity is applied results from its having a compensating effect by modifying the instrument function. This compensating effect is more marked for models G and H because of the improved fit to the extended wings of the instrument function.

As discussed in Sec. IIA it is probably more important to include Doppler broadening in the CARS model than collisional narrowing for our flame conditions (H and G, respectively, in Table I) although the differences between the best-fit temperatures are small.

The final weighted nonlinear corrected best-fit temperature of 1633 K(H), which we consider the most accurate, is 56-K hotter than the averaged Na line-reversal/thermocouple measurements of 1577 ± 20 K. Thus a discrepancy remains that cannot be explained with current available N_2 CARS models and data.

C. Stimulated Raman Pumping

The room-temperature N_2 CARS spectra frequently exhibit a small $v = 2 \rightarrow v = 1$ peak, presumably due to population of the $v = 1$ level by stimulated Raman pumping. Both the room-temperature N_2 and flame spectra were recorded using the same laser energies to monitor the amount of stimulated Raman pumping. For this reason, the necessary reduction in room-temperature N_2 IPDA signal was accomplished by inserting neutral density filters in the CARS beam rather than by attenuating the laser energies as is frequently done in CARS spectroscopy. The effect of stimulated Raman pumping, which is directly observable in room-temperature nitrogen spectra, can then be used to correlate the increase in best-fit temperature in flame spectra where the effect of stimulated Raman pumping is only indirectly observable.

In one series of experiments we deliberately defocused the laser beams, particularly the larger diam. pump beam, by inducing some spherical aberration. This produced a large increase in the stimulated Raman pumping of N_2 $v = 1$ level as shown by the experimental spectrum in Fig. 3. We characterize this pumping by measuring the ratio of the CARS $v = 2 \rightarrow v = 1$ peak amplitude (I_1) to the $v = 1 \rightarrow v = 0$ peak amplitude (I_0). We measure I_1 by visually estimating its peak height above the tail of the fundamental band. For the room-temperature N_2 spectrum in Fig. 3, the ratio $I_1{:}I_0 = 0.019$, whereas, before defocusing the laser beams, I_1/I_0 was typically 0.005.

The ratio of stimulated Raman pumping (which varies as $I_p \cdot I_s$, where I_p and I_s are the pump and Stokes laser intensities, respectively) to the CARS generation (which varies as $I_p^2 \cdot I_s$) is proportional to $1/I_p$. Thus the decrease of I_p with increasing focal spot size accounts for the increased stimulated Raman pumping of N_2 $v = 1$ level. (In practice, the total CARS signal was maintained approximately constant by increasing the pump energy but the larger focal volume resulting from the increased spot size still required a lower laser intensity, I_p.)

In fitting room-temperature or flame N_2 CARS spectra to theoretical spectra previously, no account had been taken of the population perturbation. To generate synthetic spectra to model the stimulated Raman effect, we have assumed an increased vibrational N_2 temperature (T_V), with a rotational temperature (T_R) that is independent of vibrational level and that corresponds to the kinetic temperature of the gas. This is reasonable, first, because the $\Delta J = 0, \pm 2$ selection rule for the stimulated Raman process will result in the N_2 $v = 1$ level having a similar rotational envelope to that of the ground state. Second, the rotational relaxation times τ_R are somewhat shorter than the laser pulse duration τ_L. The J dependent Raman linewidths Γ_j (FWHM) are dominated by rotational dephasing and represent the total rate of rotational energy transfer for that level:

$$\frac{\Gamma_j}{2} = \sum_{i=j} \gamma_{ij}, \tag{1}$$

where γ_{ij} is the rate of transition from state j to state i. Thus the typical rotational relaxation times of 0.18 ns at room temperature and 0.53 ns at T = 1500 K are shorter than $\tau_L \approx 10$ ns.

The vibrational relaxation times τ_v due to vibrational energy transfer are much larger than τ_L. The fastest rates occur in the hydrogen/air flame by energy transfer to water molecules[27] and for our flame conditions we estimated an N_2 vibrational relaxation time of ≈700 ns, very much longer than the laser pulse duration of ≈10 ns. Thus even under flame conditions, there is essentially no vibrational relaxation of the stimulated Raman pumped N_2 $v = 1$ level.

An instrument function was obtained from the experimental spectrum in Fig. 3 by fitting it to synthetic CARS spectra that were calculated for a fixed rotational temperature of 294 K and varying vibrational temperature. A best fit was obtained for a vibrational temperature (T_v) of 1325 K as shown in Fig. 3.

A library of synthetic CARS spectra, calculated every 50 K from 1100–2100 K, was then combined with

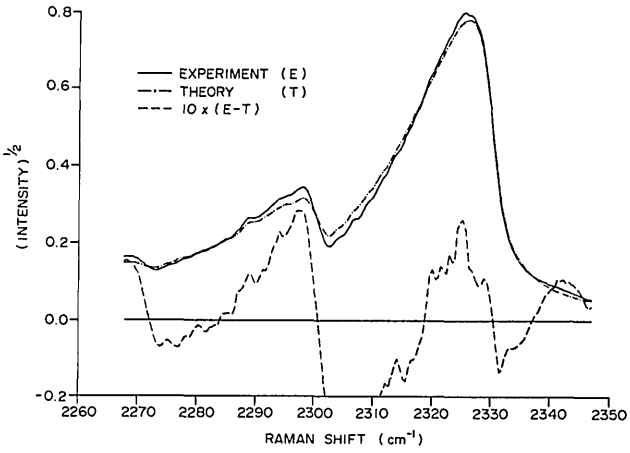

Fig. 4. Comparison of an experimental CARS flame spectrum to a best-fit theoretical spectrum (T = 1775 K) convolved with an instrument function obtained from fitting a room-temperature N_2 CARS spectrum.

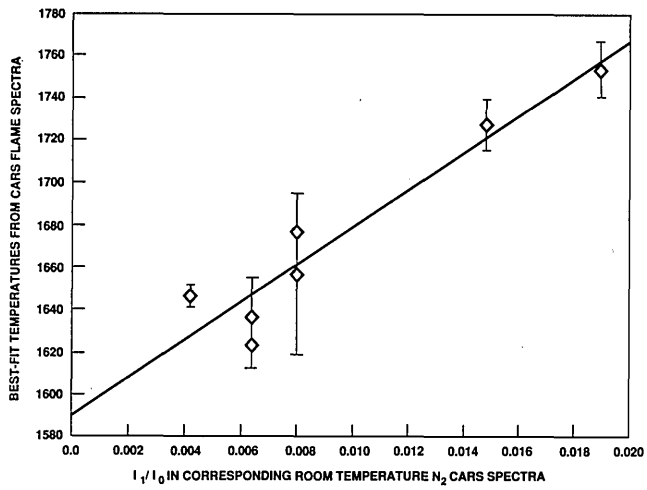

Fig. 5. Best-fit temperature for N_2 CARS flame spectra vs observed stimulated Raman pumping of N_2 v = 1 in corresponding room-temperature N_2 CARS spectrum.

this instrument function and the resulting synthetic spectra used to fit the corresponding experimental CARS flame spectra. A best fit to a 400-pulse average flame spectrum is shown in Fig. 4 where the best-fit temperature is 1775 K. The experimental spectrum is clearly vibrationally hotter and rotationally cooler than the theoretical spectrum as would be expected if population changes of the N_2 v = 1 level were occurring. The best-fit temperature is also over 100-K hotter than those recorded with tighter focusing and laser energies where the ratio I_1/I_0 is much less.

A series of experiments with varying amounts of stimulated Raman pumping in the room-temperature N_2 spectra was analyzed in a fashion similar to that described for the spectrum in Fig. 4. The results of this analysis are presented in Fig. 5 where the best-fit temperature of the flame spectrum is seen to increase with the I_1/I_0 ratio of the corresponding room-temperature N_2 spectrum.

A linear regression analysis of the data in Fig. 5 can be used to estimate the error in flame spectrum temperature measurements if the I_1/I_0 ratio of the corresponding room temperature N_2 file is known. For the data in Table I the average value of I_1/I_0 was 0.0015 and from Fig. 5 this can be seen to result in an increase of 13 K in the CARS flame temperature measurement over the temperature expected for I_1/I_0 = 0.0. Thus approximately 13 K of the 56-K discrepancy discussed in Sec. IIIB can be attributed to an increase in the v = 1 population.

To further demonstrate the presence of stimulated Raman pumping, experimental spectra were fitted with libraries of theoretical spectra that were calculated with an augmented vibrational temperature i.e., $T_V = T_R + \Delta T$ where ΔT = 0, 100, 200, 250, 300 and 400 K. The resulting best-fit variance between theory and experiment is shown in Fig. 6 as a function of N_2 vibrational temperature augmentation ΔT. The experimental spectrum is that shown in Fig. 4 for which I_1/I_0 = 0.019 and the minimum in the best-fit variance occurs for ΔT = 250 K. The resulting fit between

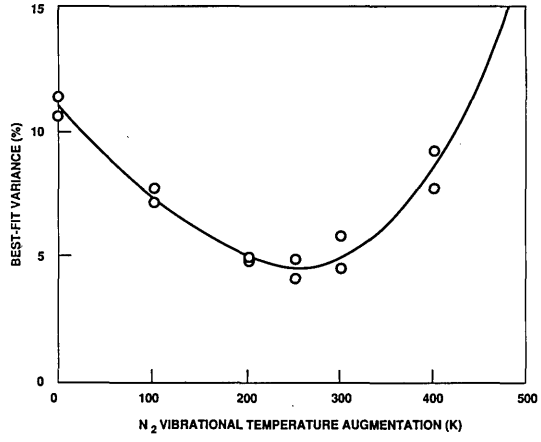

Fig. 6. Best-fit variance of the experimental flame spectrum shown in Fig. 5 (I_1/I_0 = 0.019) vs vibrational temperature augmentation ΔT. The synthetic CARS libraries were calculated for $T_V = T_R + \Delta T$ with ΔT = 0, 100, 200, 250, 300 and 400 K.

theory and experiment, which is shown in Fig. 7, is dramatically improved over that shown in Fig. 4 (for ΔT = 0). This best-fit augmentation of T_V of 250 K is greater than the observed increase in best-fit flame spectra of ≈160 K deduced from Fig. 5 for I_1/I_0 = 0.019. This is to be expected since the best fit to the flame spectrum is a compromise between fitting the vibrational and rotational envelopes as shown in Fig. 4.

We have modeled the effect of stimulated Raman pumping to see if its observed effect in room-temperature N_2 CARS spectra is consistent with the perturbations we have proposed in flame spectra. During the CARS process, perturbation of the vibrational population may occur due to stimulated Raman coupling between the two laser fields at ω_p and ω_s. This evolution of the population difference is proportional to the imaginary part of the Raman susceptibility and the product of the laser intensities $I_p \cdot I_s$, and may be expressed as[11,28]:

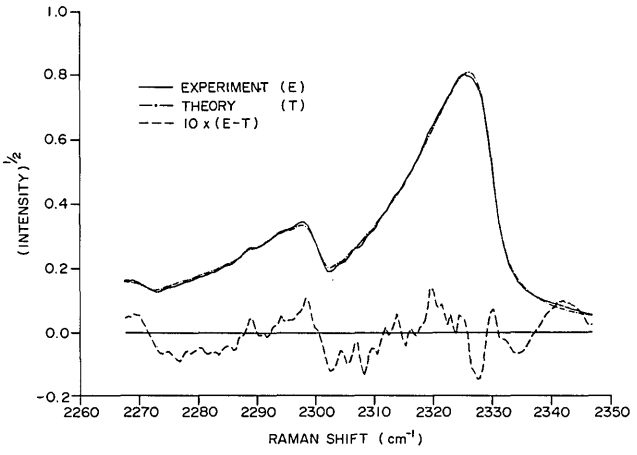

Fig. 7. Comparison of the experimental CARS flame spectrum shown in Fig. 4 to a best-fit theoretical spectrum (T_V = 1881 K; T_R = 1631 K) convolved with an instrument function obtained from fitting a room temperature N_2 CARS spectrum.

$$\frac{d(\Delta N)}{dt} = -\frac{4\pi c^4}{h\omega_s^4}\frac{d\sigma}{d\Omega}\left(\frac{4\pi}{c}\right)^2 I_p(\omega)\cdot I_s(\omega)(\Delta N)\frac{\Gamma_j}{(2\Delta\omega_j)^2+\Gamma_j^2}, \quad (2)$$

where ΔN is the population difference, $(d\sigma)/(d\Omega)$ is the Raman cross section, c is the velocity of light, h is the Planck's constant, $\Delta\omega_j$ is the detuning and Γ_j is the Raman linewidth (FWHM) for transition j.

A characteristic time τ_c for this process may be defined as

$$\tau_c^{-1} = -\frac{1}{\Delta N}\frac{d(\Delta N)}{dt} = \text{constant}\cdot g(\omega)\cdot I_p(\omega)I_s(\omega), \quad (3)$$

where

$$g(\omega) = \frac{\Gamma_j}{(2\Delta\omega_j)^2+\Gamma_j^2}, \quad (4)$$

is a Lorentzian lineshape function. For finite bandwidth sources $g(\omega)$ must be convolved with the spectral profiles of the lasers. In broadband experiments the Stokes laser has a large bandwidth and may be assumed to be constant over the region of the pump width. Thus convolution may be done with only the pump laser profile. If this latter profile is assumed to be a Lorentzian, then the convolved function $g'(\omega)$ is also a Lorentzian with a width (FWHM) equal to the sum of the Raman linewidth Γ_j and the pump bandwidth Γ_p,

$$g'(\omega) = \frac{\Gamma_j+\Gamma_p}{(2\Delta\omega_j)^2+(\Gamma_j+\Gamma_p)^2}. \quad (5)$$

If we further integrate $g'(\omega)$ over all values of detuning for a given transition,

$$\int_{-\infty}^{\infty} g'(\omega)d\omega = \pi/4$$

$$\tau_c^{-1} = I_p^o I_s \frac{4\pi c^4}{h\omega_s^4}\frac{d\sigma}{d\Omega}\left(\frac{4\pi}{c}\right)^2\frac{\pi}{4} = \alpha \quad (6)$$

where I_s is the Stokes laser intensity and I_p^o is a scaling factor for the Lorentzian pump laser intensity expression.

If we ignore the variation of $d\sigma/d\Omega$ with temperature then α, and hence τ_c, is constant with temperature.

This suggests that the characteristic time evaluated for room temperature may also be used for flame conditions provided the laser intensities remain constant.

From Eq. (2) the change in the population difference due to stimulated Raman excitation between levels v and $v+1$ is given by the rate equation,

$$\frac{d(\Delta N)}{dt} = -(\Delta N)\alpha_v - \frac{\Delta N}{\tau_D}, \quad (7)$$

where α is defined above and τ_D is the time constant for vibrational relaxation. In Eq. (6) we assume that the Raman cross section $d\sigma/d\Omega$ varies as $v+1$ [i.e., $\alpha_v = (v+1)\alpha_0$].

Since the decay of Raman-excited vibrational nitrogen ($\tau_D \approx 700$ ns) is very much slower than the laser pulse duration (τ_p = 10 ns) the term $\Delta N/\tau_D$ in Eq. (7) can be neglected. The average concentration ($\bar{N}_v$) in any vibrational level v during the laser pulse is

$$\bar{N}_v(\tau_p) = (1/\tau_p)\int_0^{\tau_p} N_v(t)dt. \quad (8)$$

We have numerically integrated the rate equations for stimulated Raman pumping of $v=0\rightarrow v=1$, $v=1\rightarrow v=2$, and $v=2\rightarrow v=3$. For the room temperature N_2 spectrum in Fig. 3, $I_1/I_0 = 0.019$, which requires a value of $\alpha_0\tau_p$ of 0.42 to produce the average population ratio of $\bar{N}_1/\bar{N}_0 = 0.080$ that is inferred from the best-fit vibrational temperature T_v = 1325 K.

This $\alpha_0\tau_p$ can then be used to predict the stimulated Raman pumping in the flame spectrum. An unperturbed N_1/N_0 of 0.122 was assumed (corresponding to T_v = 1590 K) and the rate equations were numerically integrated with this initial condition and an $\alpha_0\tau_p$ value of 0.42. The calculated value of $\bar{N}_1\bar{N}_0$ was 0.183 corresponding to a vibrational temperature of 1976 K. This is ~100-K greater than the observed best-fit vibrational temperature of 1881 K. Thus this analysis somewhat overpredicts the ratio of stimulated Raman pumping in the flame and in room temperature N_2. This may be due to approximations in the analysis, or to some defocusing of the laser beams caused by refractive index gradients in the flame.

One further piece of evidence that can be adduced to demonstrate the effect of stimulated Raman pumping is the correlation we have consistently observed between best-fit flame temperature measurements and CARS intensity. The variation in CARS intensity results from shot-to-shot variation in the focal intensities of the CARS laser beams, with the higher peak intensities expected to be associated with greater stimulated Raman pumping of N_2 $v=1$. A plot of temperature (T) for a file of 400 single-pulse CARS spectra vs spectrally integrated CARS intensity (I) and the result of a linear regression analysis of the data is shown in Fig. 8. (The corresponding averaged room-temperature N_2 spectrum has an I_1/I_0 ratio of 0.008.) The linear regression analysis gave:

$$T = (1.5\pm 0.2)I + 1603.8 \pm 6.3, \quad (9)$$

where the errors represent a single standard deviation and the average temperature was 1659 K. The intercept of Fig. 8 is consistent with that of Fig. 5, both of which should represent the best-fit temperature in the absence of any population perturbation.

The errors associated with neglecting stimulated Raman pumping and IPDA nonlinearity are partially offsetting for the data reported here. Application of the current best measurements of detector nonlinearity (Entry H, Table I) result in increase in best-fit temperature of ≈60 K (rather than the 100 K resulting from an earlier measurement that was used in the analysis of entries A–F, Table I). The stimulated Raman correction for this data reduces the best-fit flame temperatures ≈13 K. Thus application of both corrections results in a CARS temperature of 1620 K, which is 43 K greater than the Na line-reversal/thermocouple measurement.

For the data we reported previously[10] the stimulated Raman pumping was much greater than for that in Table I. The average value of I_1/I_0 was 0.005 for which the corresponding correction for stimulated Raman pumping is 45 K. This would only partially offset the effect of correcting that CARS data for detector nonlinearity.

For some CARS spectrometers, the ratio of nonresonant to resonant CARS signal was found[29,30] to increase with increasing correlation between the pump laser components, indicating non-Gaussian pump laser field statistics. With USED CARS phase matching the pump laser components are highly correlated (for the 0.69 cm^{-1} bandwidth pump laser) and if such increases occurred in our experiments they would require the use of an artificially high value of χ_{NR} to fit them.

The effect of a 50% increase in χ_{NR} can be seen by comparing C and D in Table I where the best-fit temperatures are seen to decrease by 122 K (weighted LMS fit). Thus only an 18% increase in the nonresonant CARS component would be required to explain the 43-K discrepancy between CARS and Na line-reversal/thermocouple temperature measurements in the flat-flame burner. The sensitivity of the best-fit temperatures to χ_{NR} is clearly a disadvantage of USED CARS phase matching.

D. Folded BOXCARS CARS experiments

To resolve the question of the effect of laser field statistics on CARS derived temperatures we recently repeated the CARS flame temperature measurements using folded BOXCARS phase matching with a 6.1-cm optical path difference between the pump laser components, which is greater than the 1.5-cm coherence length of the pump laser. For these uncorrelated pump laser beams no enhancement of the nonresonant CARS components is expected. For a series of seven experiments consisting of a total of 10,400 CARS flame spectra the average temperature obtained was 1594 ± 7 K, using the theory corresponding to entry H, Table I, with weighting and nonlinear correction applied. The error limit is the 95% confidence interval and does not include any estimate of possible systematic errors. The average stimulated Raman I_1/I_0 ratio for these experiments was 0.0008 (considerably lower than the corresponding USED CARS experiments), which, from Fig. 5, would result in the best-fit CARS temperature being 6-K too high. With this correction the measured CARS temperature of 1588 K is in satisfactory agreement with the Na line-reversal/thermocouple measurement of 1577 ± 20 K.

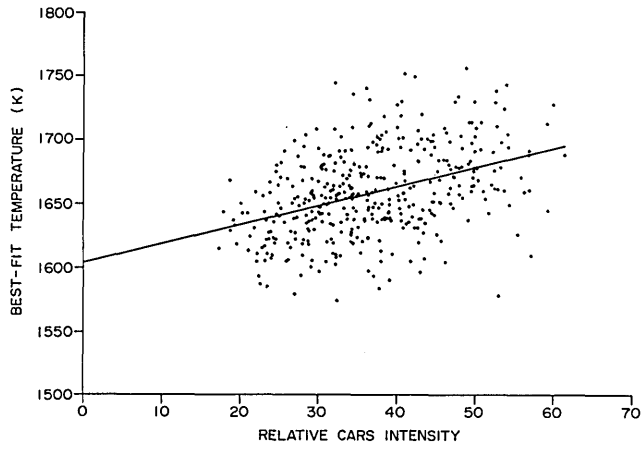

Fig. 8. Variation with relative CARS intensity of best-fit temperature for 400 single-pulse CARS spectra, and a linear regression analysis of the data.

IV. Summary and Conclusions

The typical image persistence of the IPDA detectors used in broadband CARS spectroscopy is shown to be so great that the detectors are unsuitable for single shot 10-Hz temperature measurements in turbulent combustion. This image persistence results in a CARS spectral signature that contains contributions from many previous pulses and is biased to lower temperatures. This bias is expected to be a function of the exposure history over several previous pulses. An analysis of this effect by synthesizing mixtures of two CARS spectra is shown to result in large negative errors in best-fit CARS temperatures. A prototype detector with a faster rare-earth phosphor[1] will greatly reduce this problem.

Correcting CARS spectral signatures for the recently discovered[1,2] logarithmic fall-off in IPDA sensitivity with decreasing output signal is shown to result in increases of best-fit temperature of ≈50–100 K at 1600 K. Comparisons of CARS-derived temperatures with those obtained by other techniques that have neglected this effect have claimed 1.0–1.5% accuracy. In our own work we find that the agreement previously claimed[10] was partially due to a cancelation of errors resulting from the neglect of detector nonlinearity and stimulated Raman pumping of the N_2 vibrational manifold. This may also account for the agreement observed by others.

We have demonstrated that stimulated Raman pumping can occur and we have quantitatively assessed its effect on CARS-derived temperatures. The

correlation observed between the stimulated Raman pumping of the N_2 $v = 1$ level in room-temperature N_2 spectra and the increase in best-fit temperature of the corresponding flame spectra can be used to correct for this effect. The correlation in Fig. 5 could apply to other experimental CARS configurations, provided that the room temperature N_2 spectra are recorded at the same laser intensities as the flame CARS spectra.

Rather than setting experimental conditions such as laser energy and focal spot sizes to avoid stimulated Raman pumping it is better to examine the room temperature N_2 spectra (taken at the same laser energies as the flame spectra) for the appearance of a N_2 2-1 band.

With USED CARS phase matching the correlated pump beams may have resulted in an enhanced nonresonant CARS signal. Neglecting this effect could also have partially offset the error of ignoring detector nonlinearity. Temperature measurements made using folded BOXCARS phase matching, where this effect is absent, are shown to be in good agreement with combined sodium line-reversal/thermocouple measurements when corrections for detector nonlinearity and stimulated Raman pumping are applied. Image persistence does not affect this result since the measurements were taken in a constant temperature source.

While this manuscript was in preparation, an additional study of the effect of stimulated Raman pumping on broadband CARS derived temperatures came to our attention.[2] Temperature errors of 7–8% at 1500 K were observed for the highest pump energy employed.

References

1. D. R. Snelling, G. J. Smallwood, and R. A. Sawchuk, "Nonlinearity and Image Persistence of P-20-Phosphor Based Intensified Photodiode Array Detectors used in CARS Spectroscopy," Appl. Opt. **28,** 3226–3232 (1989), same issue.
2. S. Kroll, M. Alden, P. -E. Bengtsson, and C. Lofstrom, "An Evaluation of Precision and Systematic Errors in Vibrational CARS Thermometry," J. Appl. Phys. B, to be published.
3. A. C. Eckbreth, "Optical Splitter for Dynamic Range Enhancement of Optical Multichannel Detectors," Appl. Opt. **22,** 2118–2123 (1983).
4. L. P. Goss, G. L. Switzer, D. D. Trump, and P. W. Schreiber, "Temperature and Species-Concentration Measurements in Turbulent Diffusion Flames by the CARS Technique," AIAA Publ. No. 82-0240 (1982).
5. M. Pealat, P. Bouchardy, M. Lefebvre, and J. -P. Taran, "Precision of Multiplex CARS Temperature Measurements," Appl. Opt. **24,** 1012–1022 (1985).
6. A. C. Eckbreth, "Laser Diagnostics for Combustion Temperature and Species," Abacus Press, Cambridge, MA (1988).
7. D. A. Greenhalgh, "CARS Thermometry for Low and High Pressure Combustion Systems," in *Proceedings, Sixty-Seventh AGARD Conference (No. 399) on Advanced Instrumentation for Aero Engine Components*, Philadelphia (May 1986).
8. D. A. Greenhalgh and F. M. Porter, "CARS Application in Chemical Reactors, Combustion and Heat Transfer," in *Proceedings, First International Laser Science Conference*, Dallas (November 1985).
9. F. Y. Yueh and E. J. Beiting, "Simultaneous N_2, CO, and H_2 Multiplex CARS Meaurements in Combustion Environments Using a Single Dye Laser," Appl. Opt. **27,** 3233–3243 (1988).
10. D. R. Snelling, G. J. Smallwood, R. A. Sawchuk, and T. Parameswaran, "Precision of Multiplex CARS Temperatures Using Both Single-Mode and Multimode Pump Lasers," Appl. Opt. **26,** 99–110 (1987).
11. P. R. Regnier, F. Moya, and J. P. Taran, "Gas Concentration Measurements by Coherent Raman Anti-Stokes Scattering," AIAA J. **12,** 826–831 (1974).
12. A. Gierulski, M. Noda, T. Yamamoto, G. Marowsky, and A. Slenczka, "Pump-Induced Population Changes in Broadband Coherent Anti-Stokes Raman Scattering," Opt. Lett. **12,** 608–610 (1987).
13. D. R. Snelling, R. A. Sawchuk and R. E. Mueller, "Single-Pulse CARS Noise: A comparison Between Single-Mode and Multimode Pump Lasers," Appl. Opt. **24,** 2771–2778 (1985).
14. D. R. Snelling, R. A. Sawchuk, and G. J. Smallwood, "Multichannel Light Detectors and Their Use for CARS Spectroscopy," Appl. Opt. **23,** 4083–4089 (1984).
15. A. C. Eckbreth, "BOXCARS, Crossed-Beam Phase-Matched CARS Generation in Gases," Appl. Phys. Lett. **32,** 421–423 (1978).
16. D. R. Snelling, National Research Council of Canada, unpublished results.
17. T. Parameswaran and D. R. Snelling, "The Calculation of Theoretical Coherent Anti-Stokes Raman Spectra," NRC Technical Report TR-GD-013 (1989).
18. M. L. Koszykowski, R. L. Farrow, and R. E. Palmer, "Calculation of Collisionally Narrowed Coherent Anti-Stokes Raman Spectroscopy Spectra," Opt. Lett. **10,** 478–480 (1985).
19. R. E. Teets, "Accurate Convolutions of Coherent Anti-Stokes Raman Spectra," Opt. Lett. **9,** 226–228 (1984).
20. H. Kataoka, S. Maeda, and C. Hirose, "Effects of Laser Linewidth on the Coherent Anti-Stokes Raman Spectroscopy Spectra Profile," Appl. Spectrosc. **36,** 565–569 (1982).
21. M. A. Henesian and R. L. Byer, "High Resolution CARS Line Shape Function," J. Opt. Soc. Am. **68,** 648–649 (1978).
22. J. P. Boquillon, M. Pealat, P. Bouchardy, G. Collin, P. Magre, and J. P. Taran, "Spatial Averaging and Multiplex Coherent Anti-Stokes Raman Scattering Temperature–Measurement Error," Opt. Lett. **13,** 722–724 (1988).
23. R. J. Hall, J. P. Verdieck, and A. C. Eckbreth, "Pressure-Induced Narrowing of the CARS Spectrum of N_2," Opt. Commun. **35,** 69–75 (1980).
24. L. A. Rahn and R. E. Palmer, "Studies of Nitrogen Self-Broadening at High Temperature with Inverse Raman Spectroscopy," J. Opt. Soc. Am. B **3,** 1164–1169 (1986).
25. L. A. Rahn, in *Technical Digest, Conference on Lasers and Electo-Optics* (Optical Society of America, Washington, DC, 1986), "N_2 Raman Linewidths in a H_2-O_2-N_2 Flame by Inverse Raman Spectroscopy," paper TuK 42.
26. R. L. Farrow, R. Trebino, and R. E. Palmer, "High-Resolution CARS Measurements of Temperature Profiles and Pressure in a Tungsten Lamp," Appl. Opt. **26,** 331–334 (1986).
27. J. A. Blauer and G. R. Nickerson, "A Survey of Vibrational Relaxation Rate Data for Processes Important to CO_2-N_2-H_2O Infrared Plume Radiation," Technical Report No. AFRPL-TR-73-57 (1973).
28. S. Druet and J. P. E. Taran, "CARS Spectroscopy," Prog. Quantum Electron. **7,** 1–72 (1981).
29. L. A. Rahn, R. L. Farrow, and R. P. Lucht, "Effects of Laser Field Statistics on Coherent Anti-Stokes Raman Spectroscopy Intensities," Opt. Lett. **9,** 223–225 (1984).
30. R. L. Farrow and L. A. Rahn, "Interpreting Coherent anti-Stokes Raman Spectra Measured with Multimode Nd:YAG Pump Lasers," J. Opt. Soc. Am. B **2,** 903–907 (1985).